NAIC-ID(RS)T-0613-95

NATIONAL AIR INTELLIGENCE CENTER

AN ADAPTIVE APPROACH TO OBJECT EXTRACTION AND TRACKING IN COMPLEX IMAGE SEQUENCES

by

Zhang Tianxu, Dai Kerong, Peng Jiaxiong

Approved for public release: distribution unlimited

HUMAN TRANSLATION

NAIC-ID(RS)T-0613-95 7 February 1996

MICEOFICHE NR: 96C000061

AN ADAPTIVE APPROACH TO OBJECT EXTRACTION AND TRACKING IN COMPLEX IMAGE SEQUENCES

By: Zhang Tianxu, Dai Kerong, Peng Jiaxiong

English pages: 21

Source: Dianzi Xuebao Vol. 22, Nr. 10, 1994, pp. 46-53

Country of origin: China
Translated by: SCITRAN
F33657-84-D-0165
Requester: NAIC/TASC/Richard A. Peden, Jr.
Approved for public release: distribution unlimited.

ABSTRACT Based on visual perception principles, this article studies computational models and algorithms associated with the extraction and tracking of moving targets in complex images. It analyzes and tests the effects of changing relevant model parameters on image segmentation thresholds. What is different from certain conventional algorithms is that new methods make an integrated consideration of object-background conditions, visual nonlinearities, interframe correlativity and differences into a two step integrated target extraction process including three criteria and a fast optimizing procedure. Object tracking makes use of binary template matching. Experimental results are given for visible light image sequences.

KEY WORDS Image segmentation, Object tracking, Image sequence processing, Visual perception, Adaptive system

GRAPHICS DISCLAIMER

All figures, graphics, tables, equations, etc. merged into this translation were extracted from the best quality copy available.

I. INTRODUCTION

Real time moving object extraction is an important problem in such fields as pattern recognition, image processing, machine vision, guidance, and so on. In normal tracking systems, there are two basic operations, that is, object image segmentation and correlation matching. When operating in complex image sequences and altered environmental conditions, the steadiness of these operations and the complexity of computations directly influence system performance. However, most previous research work was limited to relatively simple image sequences, thus limiting the range of applications associated with the research results. Object image segmentation methods which are normally used are based on image gray level information and include Bayesian decision making methods, White Sands target range segmentation methods, optimum entropy segmentation methods, as well as clustering criterion methods presented by Otsu, and so on [1-5]. These methods each have their advantages and applicable conditions. Existing problems are: (i) lack of capability to automatically set up appropriate segmentation windows and /47 areas; (ii) based on absolute gray or absolute gray variations, it is, therefore, very difficult, under conditions associated with complex backgrounds and environmental changes, to achieve object extraction results with steady performance. Attention is paid to the object extraction of human vision under complex background environment conditions, tracking flexibility, and adaptive performance. This article takes certain principles among these and introduces them into the study of these problems in order supply the methodological foundation to develop--in complex pictures--adaptive object extraction and tracking systems.

II. ADAPTIVE OBJECT EXTRACTION

1. Object Background Conditions

Conventional object image segmentation methods assume that areas awaiting segmentation (whole images or sub images) contain adequate object and background information. However, in a number of actual applications, these assumptions cannot be guaranteed before the fact. This creates one of the causes for unstable object extraction algorithm performance. Taking segmentation criteria put forward by Ostu as an example [4], one obtains criteria associated with optimum segmentation threshold t_0^* as

$$\sigma_b^2(t)=\omega_1(t)\omega_2(t)(m_2(t)-m_1(t))^2 \quad (1)$$

$$\sigma_{b(\max)}^2(t_0^*)=\max\{\sigma_b^2(t)\} \quad (2)$$

In the equations, threshold t takes image elements f(x,y) and divides them into object class C1 and background class C2. σ_b^2 is the variance between classes. ωj is the relative area associated with the class Cj. mj is the average degree of gray associated with the class Cj. As far as j=(1,2) is concerned, they are both functions of threshold t. max is selecting maximum value operations.

Kittler and others discovered that, in images, when the differences of ratios between objects and backgrounds are very large, 2 (t) can possibly not be a single peak. Even if it is a single 2 (max) peak, it still does not definitely correspond to accurate (segmentation result) thresholds. 1 can appear in the vicinity of average gray values associated with classes counting relatively greatly in proportions [5]. As is shown in Fig.1, in case (a), areas accounted for by object and background ω1 and ω2 are comparable. In case (b), ω1 << ω2 .

Moreover, in case (c), $\omega 2 << \omega 1$. Obviously, case (a) is the condition that any segmentation algorithm hopes to satisfy. However, in case (b), algorithms will take the relatively numerous background image elements and determine them to be targets. In case (c), algorithms can take a portion of target image elements and read them as b-ckground. This is because,

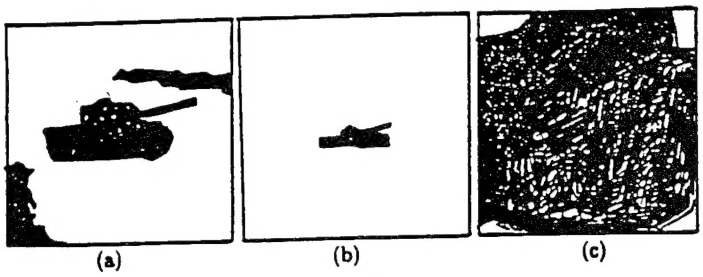

Fig.1 A Few Typical Object Background Conditions

normally, characteristic values associated with objects--such as gray values--are not absolutely uniform. The object in case (c) occupies almost the entire segmentation area. Therefore, certain nonuniform parts of objects--speaking in terms of algorithms--seem like they have changed into "object" and the remaining part seems to have changed into "background". Case (b) can be analyzed in a similar way. Therefore, Kittler and others discovered that one of the causes of this problem ought to be that, when segmentation criteria are made use of and areas have not satisfied proper conditions for object and background, segmentation algorithms with stable performance should include a step associated with the automatic discrimination and adjustment of segmentation areas. Attention is paid to human vision--in the process of apprehending pictures--being able to flexibly alter fixation points and the size of fixation areas. Fixation points

are primarily distributed in locations where information is relatively abundant and characteristics are relatively striking [6]. Taking this principle and introducing it into object extraction processes, it is possible to obtain a simple computational model associated with changing fixation points and areas in order to achieve optimum segmentation areas. Simple rational criteria for estimating whether information in a certain area is abundant or not can be intuitively deduced from Fig.1. In case (a), segmentation area characteristics such as gray variance contrasts are relatively large. However, on the basis of uniformity within classes, the variance contrasts associated with areas in cases (b) and (c) are relatively small. Letting the size of segmentation area Ω(x1,y1) be LxW, (x1,y1) is the center coordinate in the area in question. The mean value of image element f(x,y) in Ω is mo. Variance σ2 is

$$\sigma^2=\frac{1}{L\times W}\sum_{x=-L/2}^{L/2}\sum_{y=-W/2}^{W/2}(f(x_1+x,y_1+y)-m_0)^2 \tag{3}$$

$$m_0=\frac{1}{L\times W}\sum_{x=-L/2}^{L/2}\sum_{y=-W/2}^{W/2}f(x_1+x,y_1+y) \tag{4}$$

Letting L, W, and (x,y) be variables, the size and location of areas awaiting segmentation Ω can change. σ2 is a function of L, W, and (x1,y1). Because of this, criteria to find optimum segmentation areas can be written as

$$\sigma^2_{\max}(L^*,W^*\,|\,x_1^*,y_1^*)=\max_{\substack{L_0-\Delta L\le L\le L_0+\Delta L\\ W_0-\Delta W\le W\le W_0+\Delta W\\ x_0-\Delta x\le x_1\le x_0+\Delta x\\ y_0-\Delta y\le y_1\le y_0+\Delta y}}\{\sigma^2(L,W)\,|\,x_1,y_1\} \tag{5}$$

In the equations, Lo, Wo, xo, and yo are original values of variables. ΔL, ΔW, Δx, and Δy are search radii. L*, W*, (x_1^*, y_1^*) are the length, width, and position coordinates segmentation area Δ* .

2. Visual Nonlinearity and Constancy

Segmentation is the initial perception process associated with objects and backgrounds. Let Δm = Δm2 - m1Δ. Then, equation (1) can be written as

$$\sigma_b^2(t)=\omega_1(t)\omega_2(t)\Delta m^2(t) \tag{6}$$

Without losing generality, Δm can be seen as the absolute difference in brightness between object C1 possessing average brightness m1 and background C2 possessing average brightness m2 . Experiments in the biology and psychology of vision point out

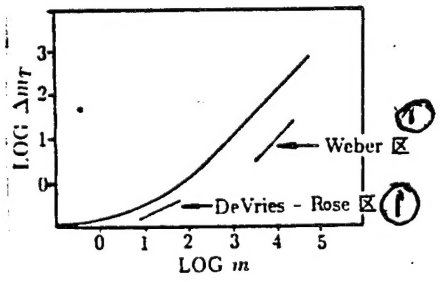

Fig.2 Relationship Between ΔmT and m

Key: (1) Zone

that, in backgrounds of different brightnesses, equal absolute differences in brightness are certainly not able to give rise to equal visual responses. Vision capabilities of distinguishing against Δm follow along with increases in background brightness m and decrease. If one uses the brightness difference ΔmT where perception is just possible to characterize this type of perception capability, then ΔmT follows increases in m and increases [7]. As is shown in Fig.2, the relationship between ΔmT and m is nonlinear. It can be divided into the dark adaptation zone, the Devries-Rose zone, and the Weber zone, being approximately represented as

$$\Delta m_T = \begin{cases} a_1 m^{1/2}, & \text{Devries-Rose 区 zone} \\ a_2 m, & \text{Weber 区 zone} \end{cases} \tag{7}$$

In the equations, a1 and a2 are appropriate constants. Obviously, criterion functions associated with equation (6) are dependent on changes in absolute degrees of gray. Therefore, they do not match up with visual nonlinearities. Besides this, equations (3) Ω (5) are average measurements of nonuniformities within Δ. Nonlinearity is also a type of brightness change. If one makes use of equations (3) - (5) as criteria, then perceptions of nonlinearity are only related to average absolute brightness changes within the area. Therefore, there exist problems of the same kind. If one takes the concept of background brightness and generalizes it to include average brightness associated with an area, then equation (3) can be revised in order to reflect visual nonlinearity principles

$$\sigma^2 = \frac{1}{L \times W} \sum_{x=-L/2}^{L/2} \sum_{y=-W/2}^{W/2} \left\{ \frac{f(x_1+x, y_1+y) - m_0}{S_0(m_0)} \right\}^2 \tag{8}$$

In equations, So(mo) is the increasing function associated with mo. For example, it is possible to select the form

$$S_0(m_0)=\begin{cases}\sqrt{\theta_1 m_0+\beta_1} & m_0<m_T\\ \theta_2 m_0+\beta_2 & m_0\geqslant m_T\end{cases} \tag{9}$$

mT is the predetermined brightness threshold. Equations (1) and (2) are revised to be

$$\sigma_b^2(t)=\omega_1(t)\omega_2(t)\{\frac{m_2(t)-m_1(t)}{S_1(m_j,m_0)}\}^2 \tag{10}$$

$$\sigma_{b\max}^2(t_1^*)=\max\{\omega_1(t)\omega_2(t)[\frac{\Delta m(t)}{S_1(m_j,m_0)}]^2\} \tag{11}$$

In the equations, S1 (mj,mo) is the increasing function associated with mj . As far as (j=1,2) are concerned, it is possible to select the forms below /49

$$S_1(m_j,m_o)=\begin{cases}\sqrt{a_1(m_j+c)+b_1} & m_0<m_T,\\ a_2(m_j+c)+b_2 & m_o\geqslant m_T\end{cases} \tag{12a}$$

(12b)

Above, the forms of So (.) and S1 set up a conceptual relationship with Devries-Rose zones and Weber zones, thereby considering, in calculations, using the parameters θ1, β1, θ2, β2 and a1, b1, a2, b2 to control the strength of the influences of mo and mj on segmentation process nonlinearities. The parameter c can be used to control the influences in changes of environmental illumination on segmentation processes. Equations (8) - (12) reflect the concepts of perceptual relative brightness changes.

During actual calculations, in the end, option is made for mj = m1 or mj = m2. As far as what sort of influence the parameters aj, bj, and c have on optimized threshold t* is concerned, it is necessary to carry out analysis and experimental research.

Comparing the differences between optimum thresholds obtained from equation (2) and equation (11)-- t_0^* and t_1^* --it is possible to prove that m1 and m2 are both monotonic increasing functions of the threshold variable t . Therefore, S1(mj,mo) is also a monotonic increasing function of t . Giving it a little thought, it is possible to know that the introduction of m1 and m2 has a tendency to make t_1^* lower than t_0^* . This is advantageous to the separation of relatively small objects from backgrounds in low contrast imagery. It is possible to prove that, when t changes, the range of changes in m1 is [0,mo]. The range of changes in m2 is [mo,255]. Letting S(mj,mo) = S_1^2 (mj,mo), consider the characteristics of weighting function 1/S(mj,mo). For example, make a1 = 1, c = 0, b1 = 1. Then, S(m1) = m1 + 1. S(m2) = m2 + 1. What Fig.3 shows is the 1/S(mj) curve. As far as 1/S(m1) is concerned, values are selected in the zone [0,mo]. For 1/S(m2), values are selected in the zone [mo,255]. Obviously, the rate of change associated with the former function as well as the range of changes are both greater than the latter. Therefore, the influence of m1 on equation (10)'s σ_0^2 and thus the influence on optimized

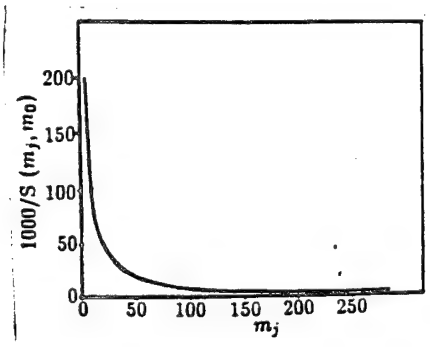

Fig.3 Weighting Function 1/S(mj)

threshold t_1^* is greater than the influence of m2. Normally, it is possible to make t_1^* drop even lower. The effects of parameter b1 is equivalent to shifting the zone of selected values associated with 1/S(mj) along the horizontal axis. When b1 increases, the zone of selected values shifts toward a location where the curve is relatively flat. The influences of the variable mj on 1/S(mj) gradually decrease. At this time, the characteristics associated with equation (11) gradually approach conventional Otsu criteria. This article designates b1 as an inertial factor. The effects of a1 lie in changing the form of 1/S(mj), thereby altering the rate of change and the scope of change, producing effects on σ_1^* . When S1 takes the form of (12-b), due to the fact that, with the same parameters, the rate of change and the scope of change associated with 1/S(mj) are generally both greater than S1 taking the form of equation (12-a), therefore, the influences of the former on t_1^* are also larger than the latter. Analysis and experiments verify that, in order to effectively take objects and separate them from backgrounds, making use of mj = m1 is often better than m2.

The brightness constancy associated with human vision systems can be represented, within a certain range, using what is shown in Fig.4 of shifts in light sensor optical strength response curves [8]. Let I stand for input light strength. R is sensor response. Rmax is maximum saturation response. K is the input optical strength corresponding to 0.5 Rmax. Then,

$$R=R_{max}(I/(I+K)) \tag{13}$$

In the Fig., response curves shift from K1 to K2. The influences of ambient optical illumination changes on whole images or local segmentation areas can use mean brightness increment Δmo for representation

$$m'_0 = m_0 + \Delta m_0, \qquad m'_j = m_j + \Delta m_0 \tag{14}$$

As a result, optical illumination changes are equivalent to shifting the 1/S(mj,mo) value selection zone, creating instability in t* values selected. Introducing parameter C to compensate for this type of change causes optimum thresholds not to be influenced by environmental changes or to be influenced very little. Environmental illumination changes are ΔI. If ΔI on whole images or local areas is approximately uniform, and the influences of these changes still lie within sensor dynamic ranges, then imagery statistical characteristic changes are reflected as left right shifts along the grayness axis in grayness histograms. After reference points have been determined beforehand, from these shifts, it is possible to calculate /50 variations of Δm_0 in equation (14). Under different conditions, in order to make imagery obtained for the same object capable--on a unified basis--of making use of standard methods to acquire segmentation results associated with stable performance, it is possible to opt for the use of standard transformations of histogram starting points to partially eliminate the effects of ΔI. For example, a transformation making the effective histogram origin to be the zero gray level operates as follows. Under certain optical illumination conditions, the histogram for

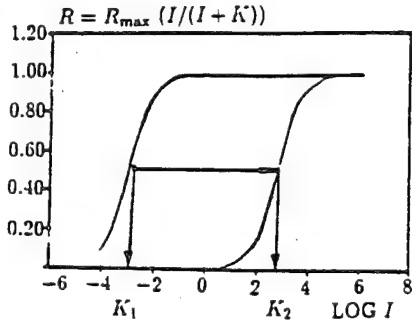

Fig.4 Optical Strength Response and Brightness Constancy

imagery obtained is p(i), i=0,1,2,...,255. Probabilities from gray level 0 to gray level k are Pk = $\sum_{\cdot}^{k} p_i(i)$. Setting up an adequately small probability threshold Δk , if Pk < Δk , then, m'j = mj - k. m'o = mo - k. After histogram transformations p'(O) = Pk , p'(i-k) = p(i), i > k. If Pk = O, then, the operations discussed above are transformations without distortion for ΔI > O. Otherwise, there is distortion. At this time, c = -k.

On the basis of the analysis discussed above, two of the causes for the problems discovered by Kittler and others ought to be Otsu segmentation criteria not possessing visual nonlinearity and constancy mechanisms. The methods in this article resolve this problem relatively well. They are capable of taking mean values associated with optimum thresholds from the vicinities of classes with relatively large surface areas and pulling them out with controllability.

3. Two Step Process Associated with Object Imagery Segmentation

Adaptive object imagery segmentation can be summarized as a process of two organically related steps.

i) On the basis of the criterion functions specified in association with equations (5), (8), and (9), optimum segmentation areas Ω are obtained.

ii) On the basis of criteria specified in association with equations (10)-(12), binary segmentation is implemented on Δ^* to solve for optimum thresholds t_i^* .

With regard to object tracking, initial windows are normally manually determined when tracking starts, or automatically determined by correlation matching times. Therefore, (x1,y1) is given. Equation (5) then simplifies to be

$$\sigma^2_{max}(L^*, W^* | x_1, y_1) = \max_{\substack{L_0-\Delta L \le L \le L_0+\Delta L \\ W_0-\Delta W \le W \le W_0+\Delta W}} \{\sigma^2(L, W | x_1, y_1)\} \qquad (15)$$

With regard to the automatic extraction of unknown small objects from large fields--because there is interest in the upper and lower limits on the sizes of object images--it is normally possible, on the basis of other information (for example, distances relative to the camera) to make rough determinations before the fact. Therefore, in equation (5), initial values associated with the size of segmentation areas and variation ranges can be set or dynamically altered in order to guarantee the relative stability of criterion characteristics concerned. Whole images are taken and divided up to be certain initial sub zones (It is permissible for parts to overlap.). Then, the center of the object must fall in a certain sub zone. The center of the sub zone in question can then act as the initial values for equation (5) coordinate variables. Coordinate variation range can be set. Because of this, it is possible to distinguish between various sub zones, using equation (5) to obtain corresponding optimum segmentation areas. Experiments verify that these methods can normally produce reasonable segmentation areas. Equation (5) is not the only criterion which can be used. Other criteria (including those possessing intelligent decision functions) are worth further study.

Equation (5) is simple and capable of recurrence calculations. The amounts of calculations added to search reasonable segmentation zones are not great. In particular, as far as the extraction of unknown objects in large fields is concerned, the amounts of calculations are primarily related to the number of sub zones. For example, with regard to 512x512 imagery, use is made of 32x32 initial sub zones on VAX11-730 computers. The time to carry out target extraction is approximately 6 seconds. Making further use of inherent parallel characteristics in the method, it will possess real time application potential.

4. Experimental Results

Experiments were carried out on microcomputer image processing systems. Fig.5 is segmentation results associated

with making use of Otsu criteria on a few images. In it, (a) and (b) are original object images and their histograms. (c) and (d) are segmentation results as well as curves for variations of σ_t^2 as a function of threshold t . (e), (f), (g), and (h) are actual results for a different image. It can be seen that, due to the fact that whole images do not satisfy appropriate object background conditions, objects of interest are not able to be separated from backgrounds. (i) is sub zones. Although they basically satisfy appropriate object background conditions, except for one image, in the other two images, there is still no capability to obtain accurate results. Fig.6 (a) and (b) are test results associated with the methods of this article. They are clearly superior to conventional methods. In experiments, we set the initial window size as 50x50. The optimum window sizes obtained for searches of two images were, respectively, 37x37 /51 and 70x70. When control parameter b1 values increase, σ_t^2 (t) curve variations are seen in (c) and (d) respectively. Obviously, optimum thresholds t_1^* ` follow increases in b1 and increases. In conjunction with this, there is an approximation of conventional Otsu criteria thresholds.

III. SEQUENCED IMAGE OBJECT EXTRACTION AND TRACKING

1. Fast Threshold Estimates

In order to increase calculation speeds associated with sequenced image object extraction, it is necessary to adequately

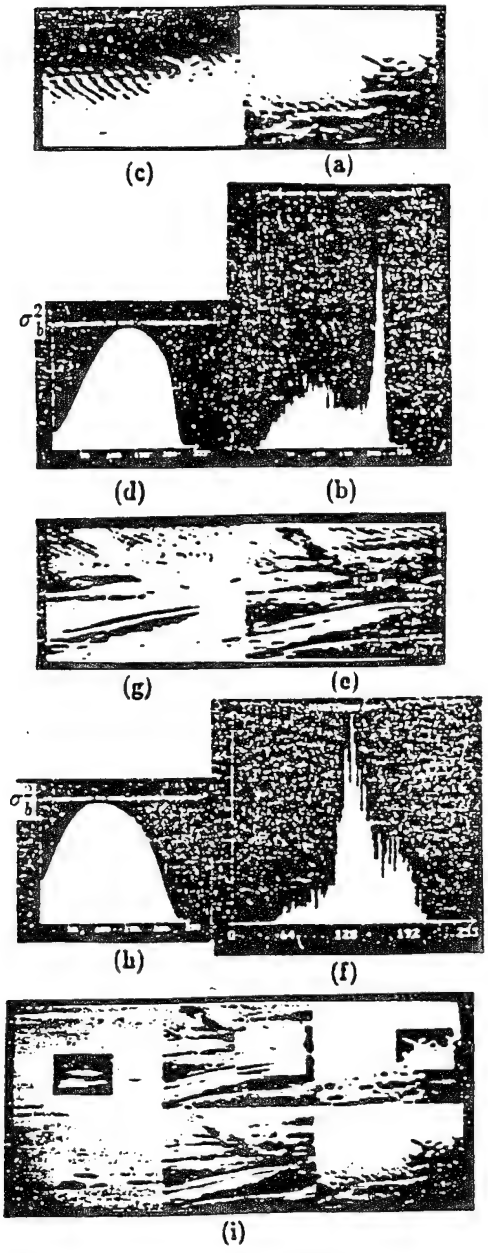

Fig.5 Conventional Method Experimental Results

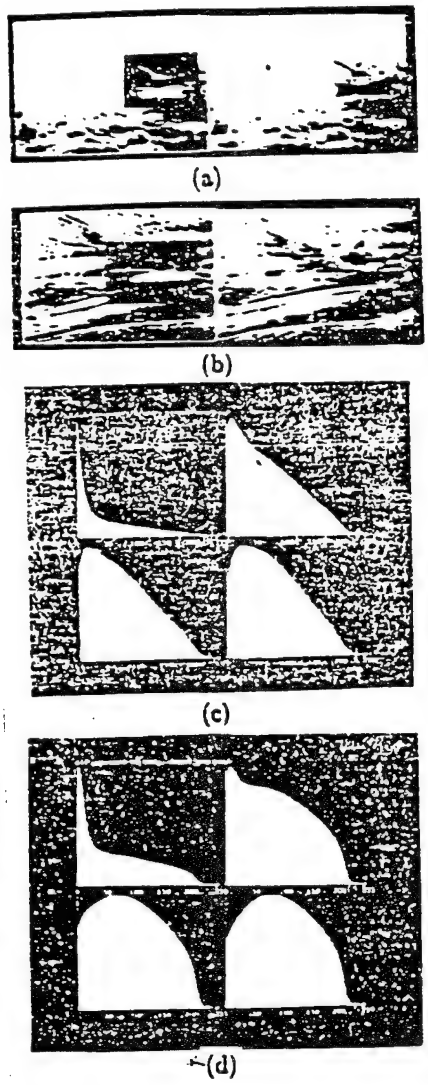

Fig.6 Experimental Results for the Methods of This Article

make use of interframe correlativities. However, object extraction and tracking in actual environments still /52 require considering differences between frames created by various types of interference and changes. Letting the statistical histogram associated with the segmented window of the previous frame be pn-1 (i), the statistical histogram of the current frame area awaiting segmentation is pn(i), i=0,1,2,...,255. Then, the relationship between the statistical characteristics of the two frames can be expressed as

$$p_n(i)=p_{n-1}(i)+\Delta p(i) \tag{16}$$

$$\sum_{i=0}^{255}\Delta p(i)=0 \tag{17}$$

In the equations, Δp(i) stands for changes in statistical characteristics between frames. As far as σ_b^2 (t) changes given rise to by Δp(i) are concerned, they lead to variations in optimum thresholds associated with various frames.

$$\sigma_b^2(t)^{(n)}=[\omega_1^{(n-1)}+\Delta\omega_1][\omega_2^{(n-1)}+\Delta\omega_2][\frac{m_2^{(n-1)}+\Delta m_2-m_1^{(n-1)}-\Delta m_1}{S_1(m_j^{(n-1)}+\Delta m_j, m_0^{(n-1)}+\Delta m_0)}]^2 \tag{18}$$

$$=\sigma_b^2(t)^{(n-1)}+\Delta\sigma_b^2(t)$$

$$t_1^*(n)=t_1^*(n-1)+\Delta t_1^* \tag{19}$$

In the equations, the superscripts n and n-1 stand for the present frame and the previous frame. Making use of interframe correlativity, the optimum threshold t*(n-1) associated with the (n-1)th frame can act as the predicted value for optimum threshold estimates associated with the nth frame window. Therefore, optimizing processes do not need to be carried out in the entire

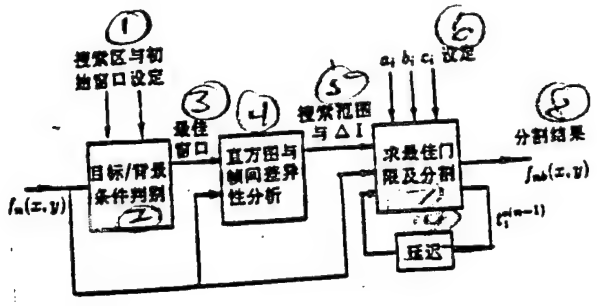

Fig.7 Object Extraction Model Schematic

Key: (1) Search Area and Initial Window Settings (2) Object/Backgroundy Condition Differentiation (3) Optimum Window (4) Histogram and Interframe Difference Analysis (5) Search Range and ΔI (6) Setting (7) Solving for Optimum Thresholds and Segmentation (8) Segmentation Results (9) Delay

gray range. However, at this time, the determination of the search range must consider interframe differences. The definition of the criterion function ϵ associated with the measurement of differences is

$$\epsilon=\sum_{i=0}^{255}|\Delta p(i)| \qquad (20)$$

Obviously, the larger ϵ is, the larger search range Δt should be. We have

$$\Delta t=h(\epsilon) \qquad t_1^{*(n)}\in[t^{*(n-1)}-\Delta t, t^{*(n-1)}+\Delta t] \qquad (21)$$

In equations, $h(\epsilon)$ is an increasing function of ϵ. At this

point, in Fig.7, this article presents an adaptive sequenced image object extraction model possessing controllability.

2. Binary Template Matching

One type of often used algorithm associated with object tracking is template matching. Here, templates are objects in previous frame tracking windows, and matching searches are then

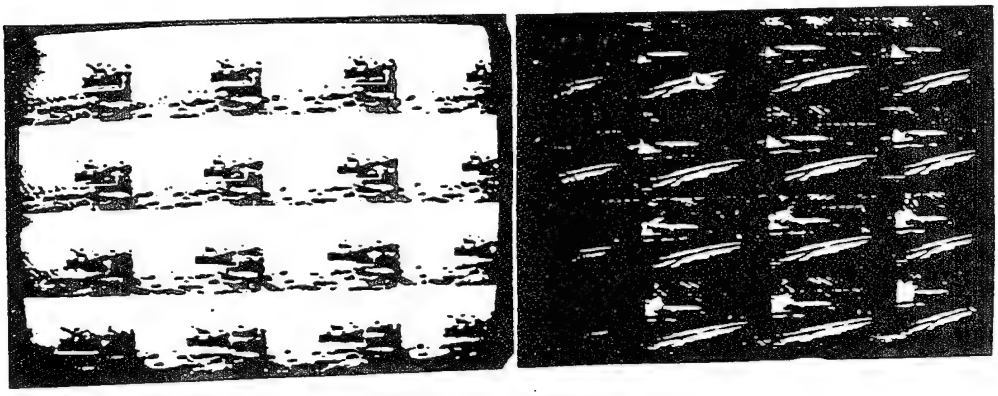

Fig.8 Sequenced Image Object Tracking Results

carried out within an area of specially designated size inside/53 the current frame, acquiring the optimum object center position within the area in question. Gray level template matching is an often used matching method, despite the fact that there are various types of fast algorithms [9-11]. However, direct gray level template matching does not possess stability with regard to environmental optical illumination conditions and interference. On the foundation of object extraction which this article has already described previously, option is made for the use of binary template matching. Search areas also make use of previously discussed two step segmentation processes to acquire binary characteristic imagery. The object extraction methods of

this article possess relatively good adaptability with regard to environmental and background changes, providing a foundation for the reliability of subsequent binary matching operations. Moreover, binary matching calculations are realized with simple and easy to use specialized hardware, possessing real time application value. Experiments are carried out on microcomputer imagery processing systems. Table 1 is partial results obtained with optimal threshold sequences during object extraction and tracking on three image series. In them, partial tracking results for the first two series of images are shown in Fig.8. From right to left and from top to bottom, the objects in sequenced images move from right to left. Tracking windows are formed automatically. Tracking results are very good.

Table 1 Optimal Threshold Sequences

图象序列	1	2	3	4	5	6	7	8	9	10	11	12	13	14	15	16
I	8	9	7	7	7	5	6	6	7	7	7	7	6	6	7	6
I	70	72	71	70	71	71	70	70	70	56	56	56	58	59	58	57
I	11	10	10	10	11	11	11	10	11	11	11	10	11	11	10	11

(1) Image Sequence

IV. CONCLUSIONS

This article analyzes certain problems associated with conventional object extraction and tracking algorithms, pointing out that the causes of instability in object extraction algorithm performance lie in not possessing differentiation and adjustment capabilities with regard to object background conditions. Moreover, they are normally based on absolute gray levels or absolute gray level changes. On the basis of visual perception principles, we put forward one type of effective sequenced image object extraction model and algorithm, analyzing and empirically demonstrating the effects of control parameters in models on segmentation threshold selection and segmentation performance. Making use of sequenced image interframe correlativity and differences, it is possible to automatically set up initial values and search ranges associated with threshold estimates. On this foundation, binary template matching and tracking are carried out. In experiments on sequenced visible light images possessing complex backgrounds, verification is done of the accuracy and broad application value of this article's methods.

REFERENCES

1 A. L. Gilbert et al. A real-time video tracking system. IEEE Trans. Pattern Anal. Machine Intell. ,1980,2(1):47—56

2 J. B. Jordan and L. C. Ludeman. Image Segmentation Using Maximum Entropy Techniques. Proc. of ICASSP'84,vol. 2,pp. 32. 4. 1—4

3 W. B. Schaming. Adaptive gate multifeature Bayesian statistical tracker. Proc. of SPIE, 1982, 359:68—76

4 N. Otsu. A threshold selection method from gray level histograms. IEEE Trans. ,Syst. Man Cybern. 1979,9(1):62—66

5 J. Kittler and J. Illingworth. On threshold selection using clustering criterion,IEEE Trans. Syst. Man Cybern. ,1985,15(5):652—655

6 H. L. Kundel and C. F. Nodine. A visual concept shapes image perception. Radiology, Feb, 1983, 146:363—368

7 G. Buchsbaum. An analytical derivation of visual nonlinearity. IEEE Trans. Biomed. Engin., 1980,27(5):237—242

8 J. Skrzypek. Lightness constancy: connectionist architecture for controlling sensitivity. IEEE Trans. Syst. Man Cybern. ,1990,20(5):957—968

9 D. I. Barnea and H. E. Silverman. A class of algorithms for fast digital image registration, IEEE Trans,Comput. ,1972,21(2):179—186

10 张天序,彭磊雄. 关于模板匹配优化的一般理论和方法. 电子学报,1987,15(3):79—88

11 张天序,吕维雪. 数字减影中的自适应位移估计. 电子学报,1991,19(5):27—34

(下转 p72)

DISTRIBUTION LIST

DISTRIBUTION DIRECT TO RECIPIENT

ORGANIZATION	MICROFICHE
B085 DIA/RTS-2FI	1
C509 BALL0C509 BALLISTIC RES LAB	1
C510 R&T LABS/AVEADCOM	1
C513 ARRADCOM	1
C535 AVRADCOM/TSARCOM	1
C539 TRASANA	1
Q592 FSTC	4
Q619 MSIC REDSTONE	1
Q008 NTIC	1
Q043 AFMIC-IS	1
E404 AEDC/DOF	1
E410 AFDTC/IN	1
E429 SD/IND	1
P005 DOE/ISA/DDI	1
1051 AFIT/LDE	1
PO90 NSA/CDB	1

Microfiche Nbr: FTD96C000061
NAIC-ID(RS)T-0613-95